

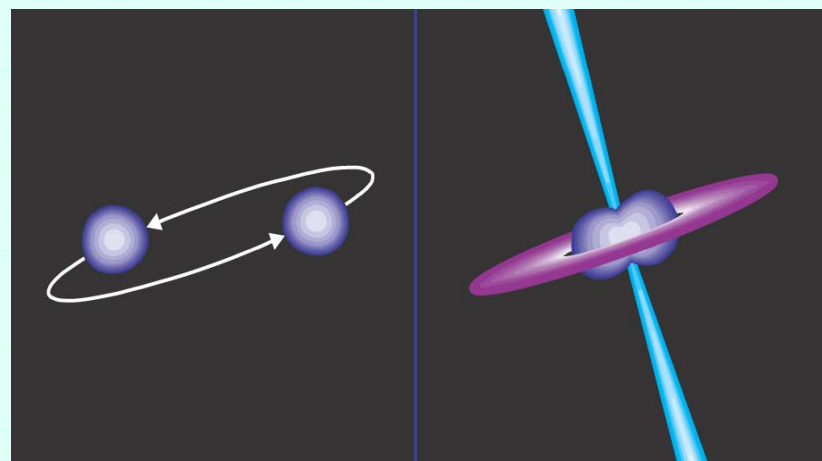
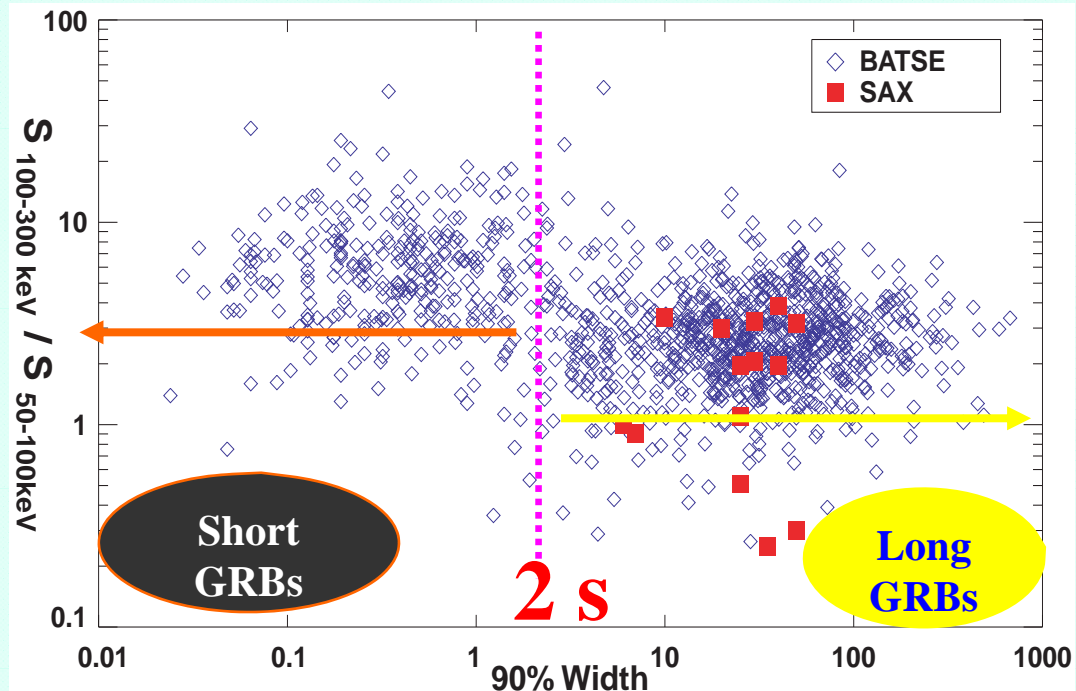
Plateau phase in X-ray afterglows of GRBs and application in cosmology

Y.-F. Huang (黄永锋)
Nanjing University (南京大学)

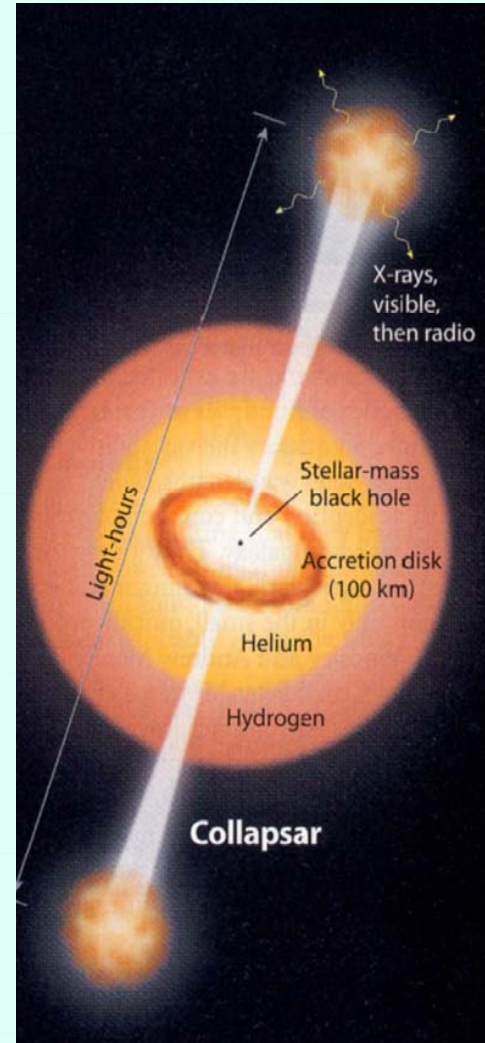
Collab.: Geng J.J., Tang C.H., Zhang Z.B., Xu M., Xu F.
合作者: 耿金军、汤晨涵、张志彬、徐明、许帆

Outline

- 1. Background**
2. Three parameter relation of plateaus
3. Application in cosmology



双中子星合并模型



塌缩星模型

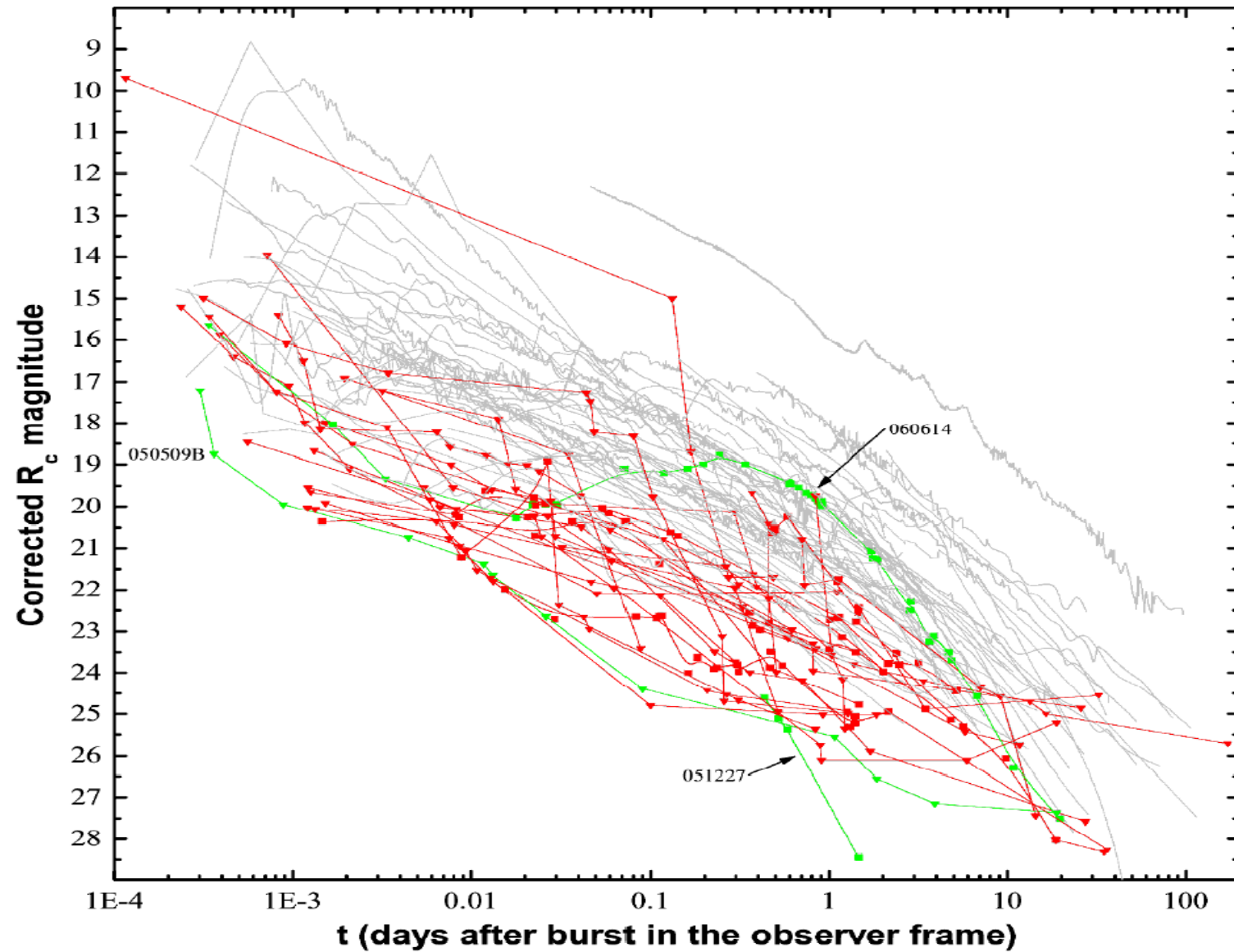
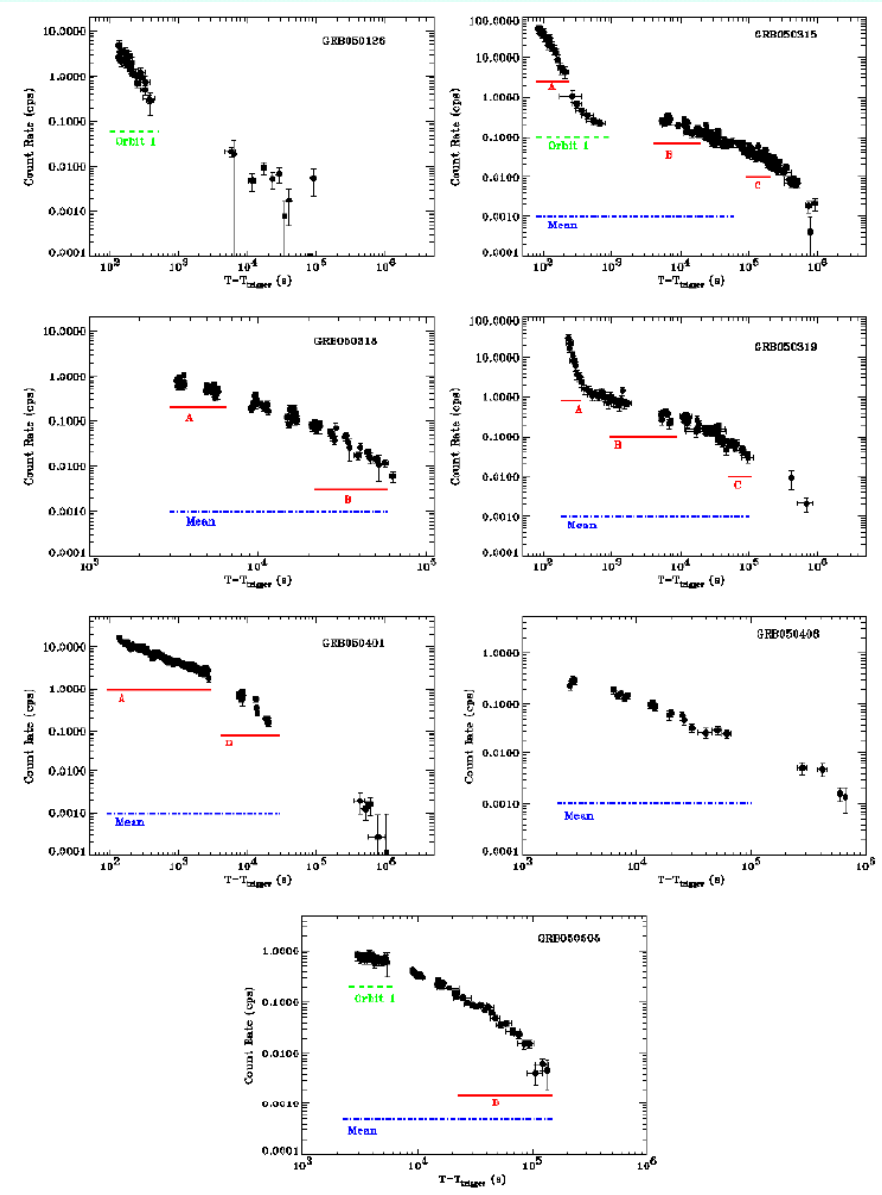


Fig. 1.— The afterglows of Type I and Type II GRBs in the observer frame. All data have been corrected for Galactic extinction and, where possible, the contribution of the host.

X-ray afterglows



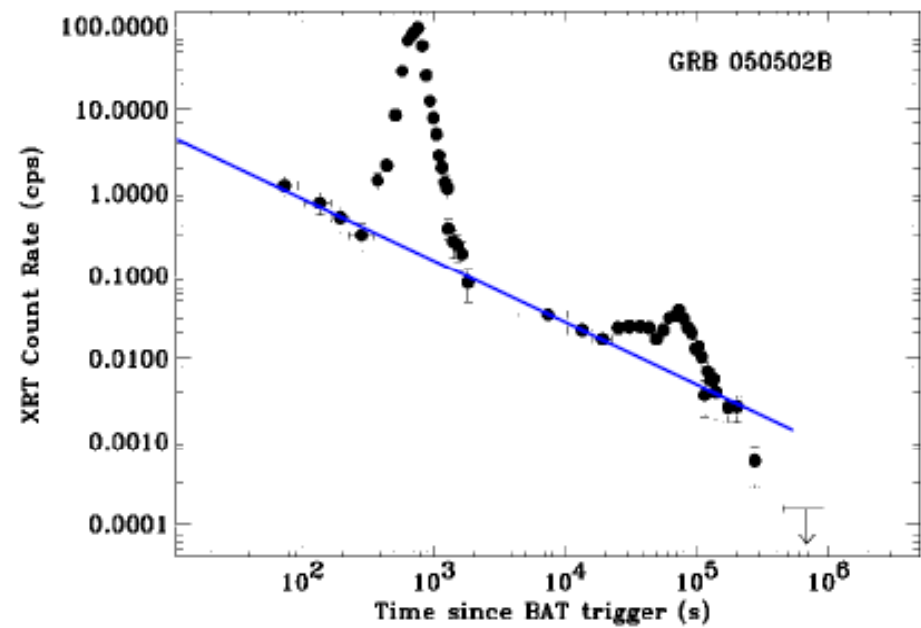
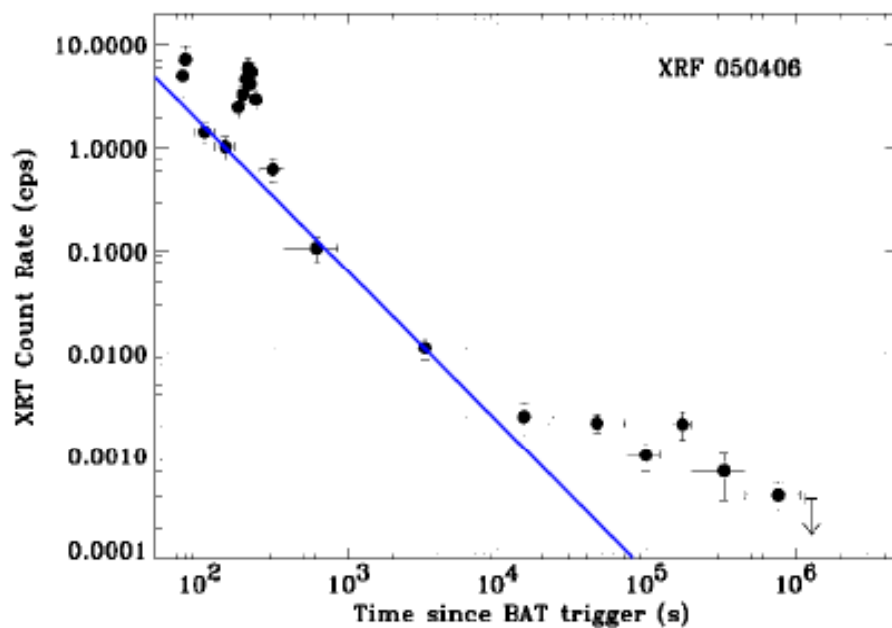
Tagliaferri et al. 2005, Nature, 436, 985 (also see Chincarini et al. 2005)

Initial steep decay: tail emission from relativistic shocked ejecta, e.g. curvature effect (Kumar & Panaitescu 2000; Zhang et al. 2006)

Flattening: continuous energy injection (Dai & Lu 1998a,b; Dai 2004; Zhang & Meszaros 2001; Zhang et al. 2006; Nousek et al. 2006; Yu & Dai 2006), implying long-lasting central engine

Final steepening: forward shock emission

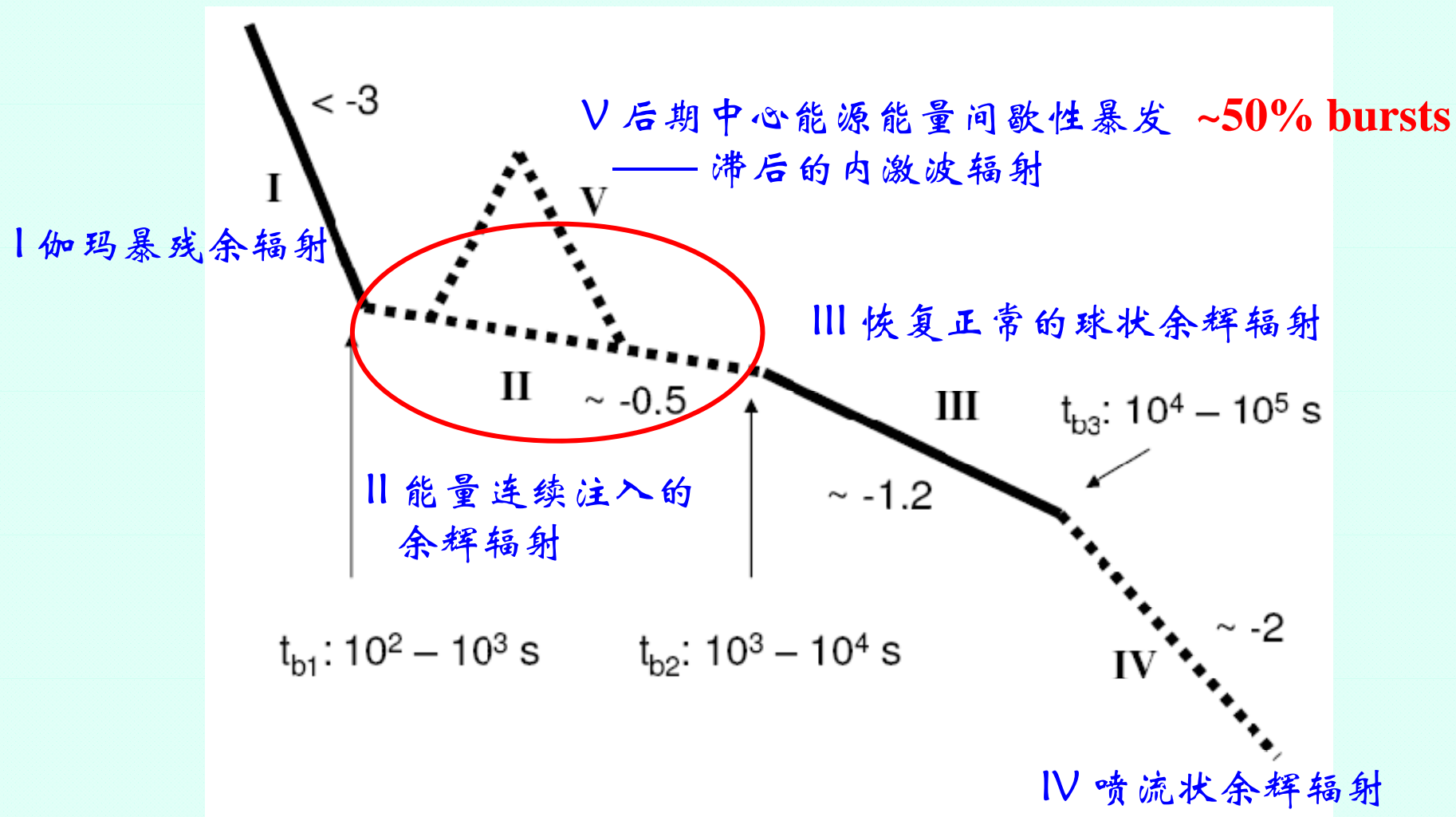
X-ray flares



Burrows et al. 2005, Science, 309, 1833

Explanation: late internal shocks (Fan & Wei 2005; Zhang et al. 2006; Wu et al. 2006), implying long-lasting central engine.

Various components in the X-ray lightcurve



Zhang et al. 2006; Nousek et al. 2006

Zhang, Fan, Dyks et al. 2006, ApJ, 642, 354

Outline

1. Background

2. Three parameter relation of plateaus

3. Application in cosmology

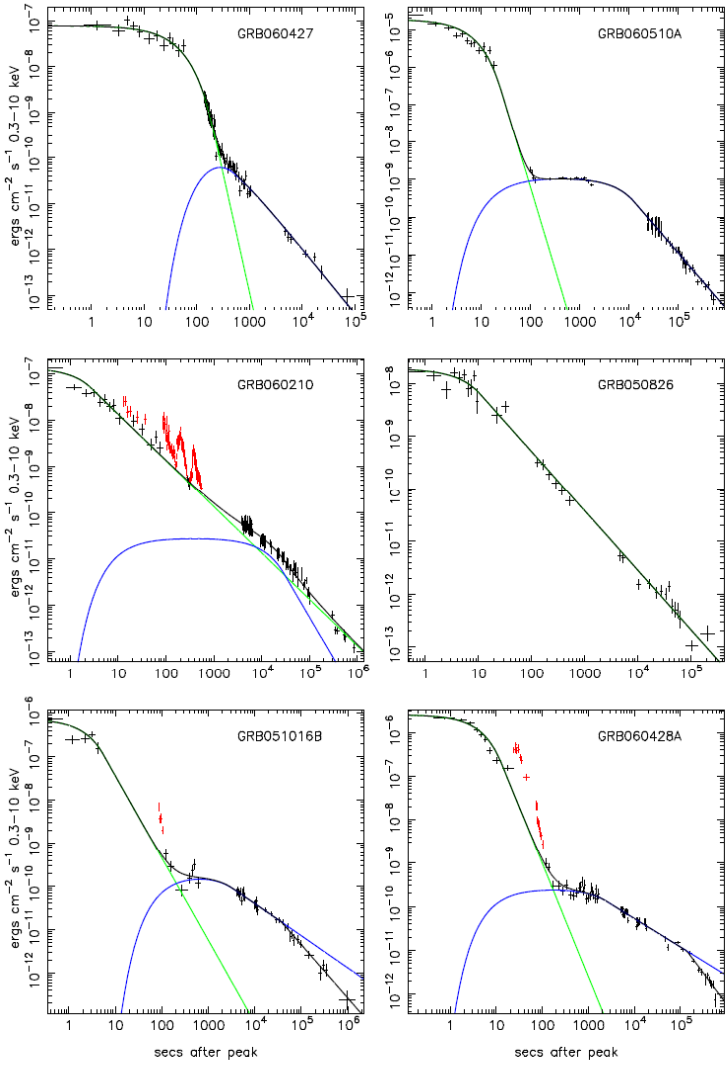
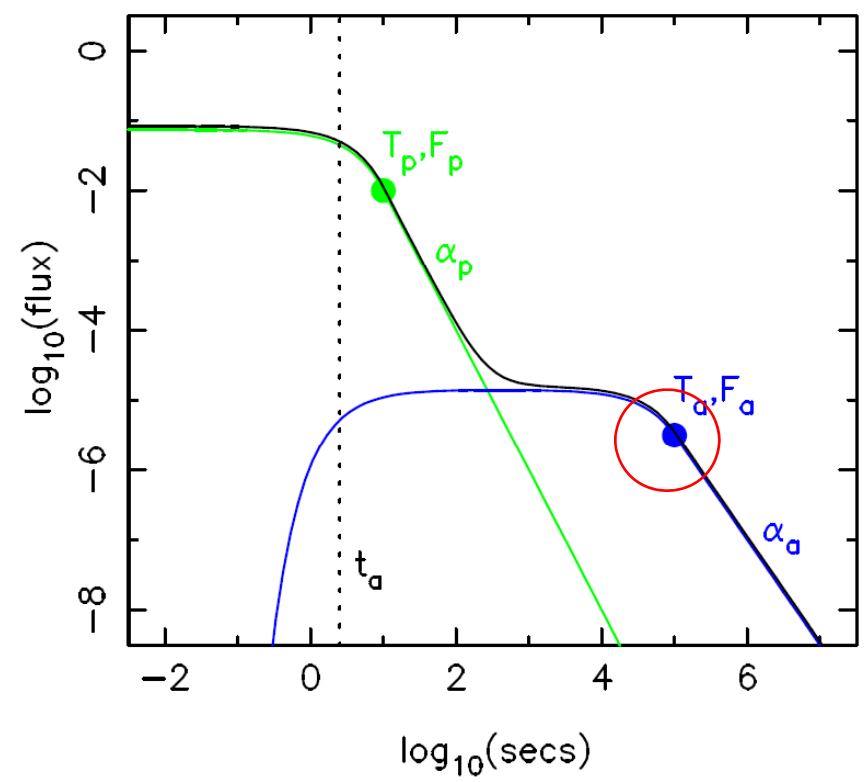


Fig. 2.— Examples of the fits to X-ray decay curves. The prompt and afterglow component functions are plotted in the same way as in Fig. 1. Top panels: the most common type in which the 2nd, afterglow, component dominates at late times. Middle panel left: a two component fit in which the afterglow component forms a bump in the decay but the extrapolation of the prompt component decay dominates at late times. Middle panel right: a single component fit, requiring no afterglow component. Bottom panels: two examples of fits which include a late temporal break. Flares are plotted in red and were excluded from

现象学描述

$$f_c(t) = \begin{cases} F_c \exp\left(\alpha_c - \frac{t\alpha_c}{T_c}\right) \exp\left(\frac{-t_c}{t}\right), & t < T_c \\ F_c \left(\frac{t}{T_c}\right)^{-\alpha_c} \exp\left(\frac{-t_c}{t}\right), & t \geq T_c \end{cases}$$

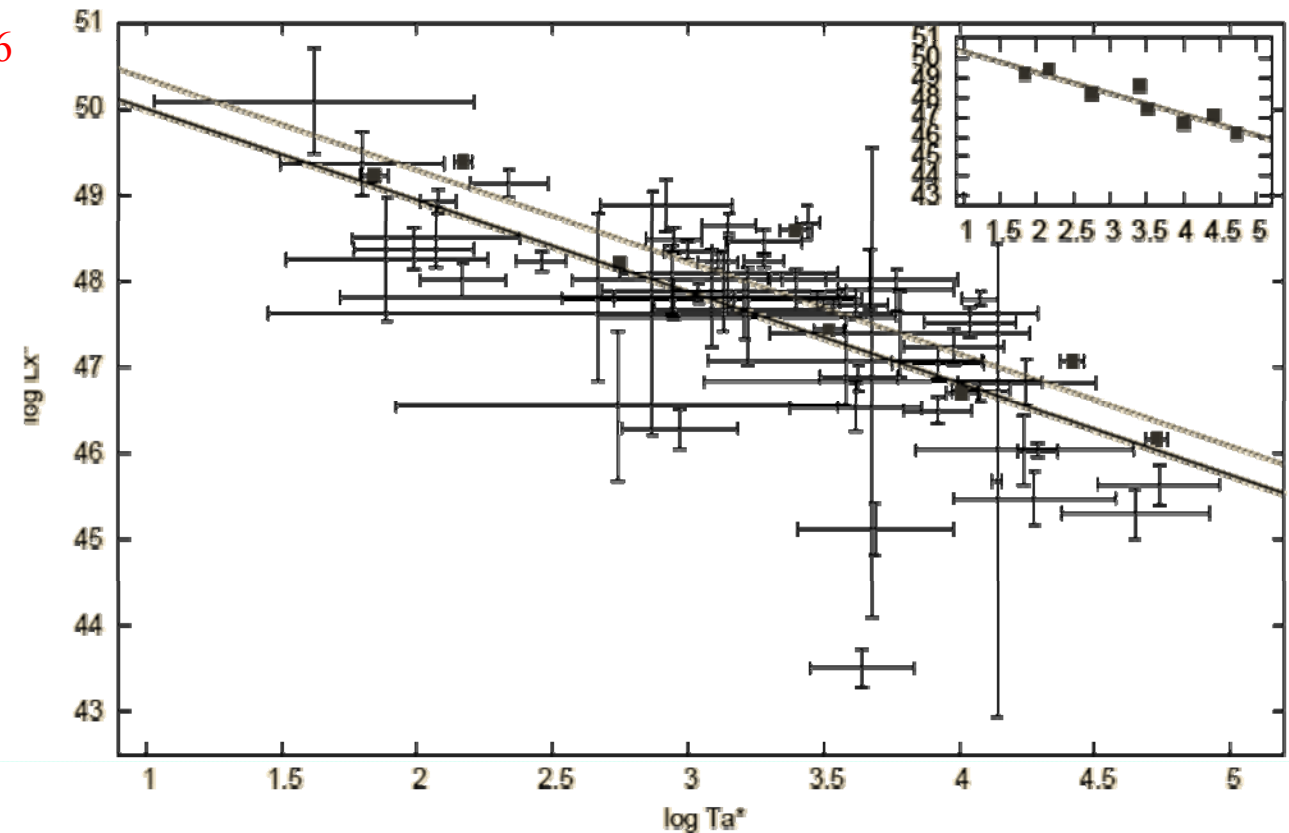


Willingale et al. 2007

LT CORRELATION

$$L_X^* \propto T_a^{*-1.06}$$

$$L_X^* = \frac{4\pi D_L^2(z) F_X}{(1+z)^{1-\beta_u}}$$



$$\log L_X^* = \log a + b \cdot \log T_a^*$$

$$\log a = 51.06 \pm 1.02 \text{ and } b = -1.06^{+0.27}_{-0.28}$$

$$T_a^* = T_a / (1+z)$$

Dainotti et al. 2010

L-T-E

55 GRBs (47个长暴8个中间类型暴)
具有红移及明显平台相

$$\log\left(\frac{L_X}{10^{47}\text{erg/s}}\right) = a + b \log\left(\frac{T_a}{10^3\text{s}}\right) + c \log\left(\frac{E_{\gamma,\text{iso}}}{10^{53}\text{erg}}\right)$$

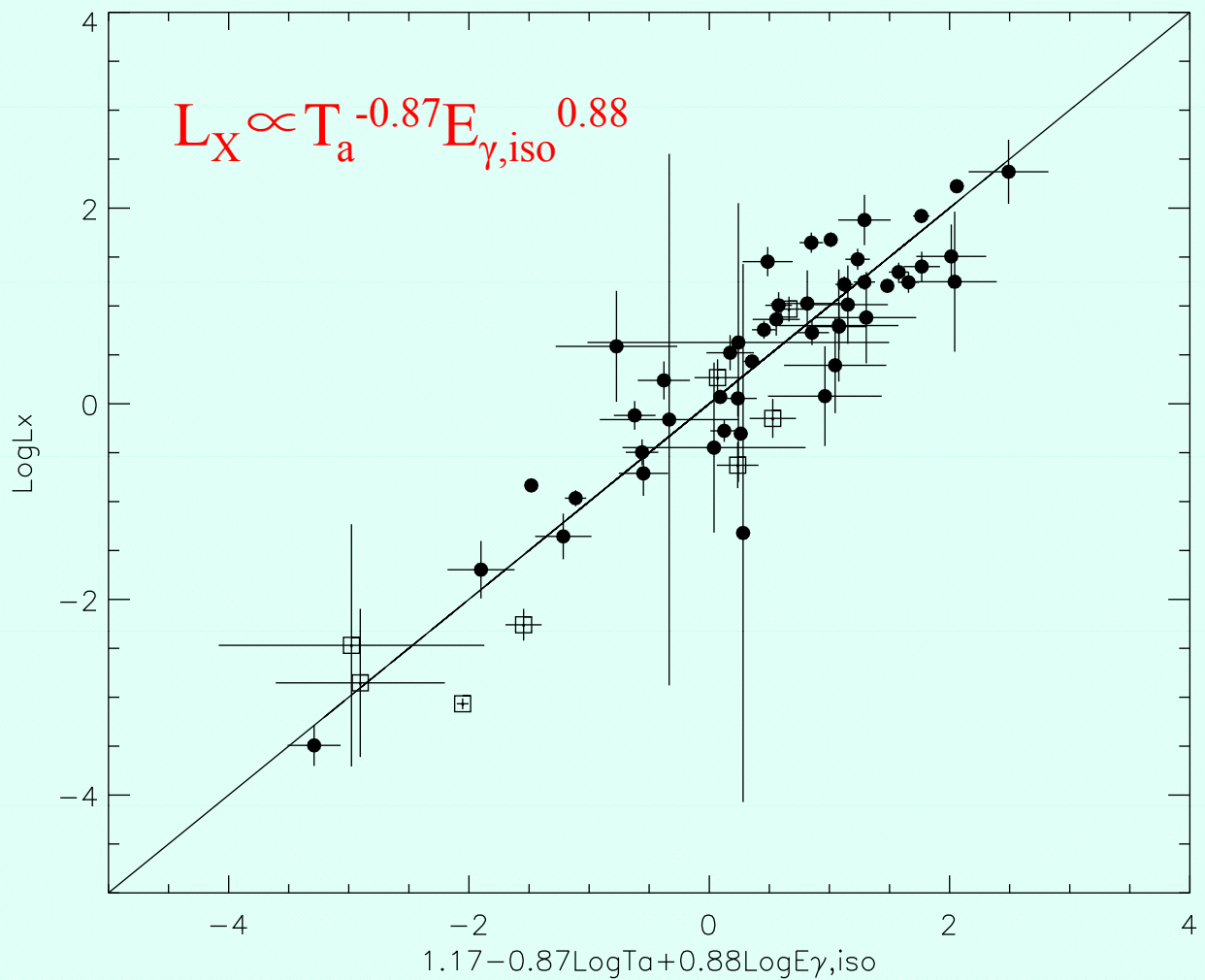
MCMC
D'Agostini 2005

$$\mathcal{L}(a, b, c, \sigma_{int}) \propto \prod_i \frac{1}{\sqrt{\sigma_{int}^2 + \sigma_{y_i}^2 + b^2 \sigma_{x_{1,i}}^2 + c^2 \sigma_{x_{2,i}}^2}} \\ \times \exp\left[-\frac{(y_i - a - bx_{1,i} - cx_{2,i})^2}{2(\sigma_{int}^2 + \sigma_{y_i}^2 + b^2 \sigma_{x_{1,i}}^2 + c^2 \sigma_{x_{2,i}}^2)}\right],$$

Xu & Huang 2011

GRB	z	$\log[L_X / (\text{erg/s})]$	$\log[T_a / (\text{s})]$	$\log[E_{\gamma,\text{iso}} / (\text{erg})]$	Type
050315	1.95	47.05 ± 0.19	3.92 ± 0.17	52.85 ± 0.012	Long
050319	3.24	47.52 ± 0.18	4.04 ± 0.17	52.90 ± 0.057	Long
050401	2.9	48.45 ± 0.15	3.28 ± 0.14	52.50 ± 0.098	Long
050416A	0.65	46.29 ± 0.23	2.97 ± 0.21	51.02 ± 0.027	Long
050505	4.27	48.03 ± 0.34	3.67 ± 0.33	53.26 ± 0.019	Long
050724	0.26	44.53 ± 1.24	4.92 ± 1.22	50.17 ± 0.055	IC
050730	3.97	48.68 ± 0.07	3.44 ± 0.04	53.26 ± 0.017	Long
050801	1.38	47.86 ± 0.17	2.17 ± 0.16	51.49 ± 0.066	Long
050802	1.71	47.43 ± 0.06	3.52 ± 0.06	52.59 ± 0.021	Long
050803	0.42	46.55 ± 0.87	2.74 ± 0.81	51.46 ± 0.069	Long
050814	5.3	47.88 ± 0.47	3.13 ± 0.45	53.29 ± 0.029	Long
050824	0.83	45.30 ± 0.29	4.65 ± 0.27	51.13 ± 0.052	Long
050922C	2.2	48.92 ± 0.07	2.08 ± 0.07	52.77 ± 0.009	Long
051016B	0.94	47.59 ± 0.57	3.22 ± 0.55	51.01 ± 0.034	Long
051109A	2.35	48.01 ± 0.13	3.4 ± 0.11	52.72 ± 0.018	Long
051109B	0.08	43.51 ± 0.21	3.64 ± 0.19	48.55 ± 0.064	Long
051221A	0.55	44.74 ± 0.16	4.51 ± 0.16	51.40 ± 0.014	IC
060108	2.03	46.50 ± 0.13	3.92 ± 0.13	51.94 ± 0.027	Long
060115	3.53	47.80 ± 0.57	3.09 ± 0.55	52.99 ± 0.023	Long
060116	6.6	49.37 ± 0.33	1.8 ± 0.3	53.33 ± 0.082	Long
060202	0.78	45.64 ± 0.23	4.74 ± 0.23	52.00 ± 0.040	Long
060206	4.05	48.65 ± 0.10	3.15 ± 0.1	52.79 ± 0.013	Long
060502A	1.51	47.27 ± 0.19	3.85 ± 0.21	52.59 ± 0.012	IC
060510B	4.9	47.39 ± 0.49	3.78 ± 0.48	53.64 ± 0.011	Long
060522	5.11	48.51 ± 0.33	2.07 ± 0.31	53.05 ± 0.026	Long
060604	2.68	47.24 ± 0.19	3.98 ± 0.18	52.21 ± 0.069	Long
060605	3.8	47.76 ± 0.09	3.48 ± 0.08	52.66 ± 0.034	Long
060607A	3.08	45.68 ± 2.75	4.14 ± 0.02	53.12 ± 0.012	Long
060614	0.13	43.93 ± 0.05	5.01 ± 0.05	51.32 ± 0.006	IC
060707	3.43	48.01 ± 0.40	2.94 ± 0.36	52.93 ± 0.025	Long
060714	2.71	48.22 ± 0.08	3.11 ± 0.07	53.06 ± 0.016	Long
060729	0.54	46.17 ± 0.04	4.73 ± 0.04	51.69 ± 0.021	Long
060814	0.84	46.69 ± 0.06	4.01 ± 0.06	52.97 ± 0.004	Long
060906	3.69	47.73 ± 0.13	3.62 ± 0.12	53.26 ± 0.042	Long
060908	2.43	48.24 ± 0.11	2.46 ± 0.09	53.03 ± 0.010	Long
060912A	0.94	46.37 ± 0.23	2.97 ± 0.18	51.91 ± 0.020	IC
061121	1.31	48.35 ± 0.10	3 ± 0.09	53.47 ± 0.004	Long
070110	2.35	48.25 ± 0.72	1.89 ± 0.37	52.90 ± 0.033	Long
070208	1.17	46.88 ± 0.15	3.63 ± 0.14	51.58 ± 0.060	Long
070306	1.49	47.07 ± 0.05	4.42 ± 0.04	53.18 ± 0.008	Long
070506	2.31	47.63 ± 1.42	2.87 ± 1.42	51.82 ± 0.029	Long
070508	0.82	48.20 ± 0.02	2.75 ± 0.02	53.11 ± 0.004	Long
070529	2.5	48.40 ± 0.15	2.34 ± 0.15	53.04 ± 0.025	Long
070714B	0.92	46.85 ± 0.20	3.03 ± 0.19	52.30 ± 0.033	IC
070721B	3.63	47.08 ± 0.51	3.58 ± 0.51	53.34 ± 0.035	Long
070802	2.45	46.84 ± 2.72	3.68 ± 0.62	51.96 ± 0.047	Long
070809	0.22	44.15 ± 0.76	4.09 ± 0.75	49.43 ± 0.062	IC
070810A	2.17	47.97 ± 0.13	2.83 ± 0.12	52.26 ± 0.023	IC
071020	2.15	49.22 ± 0.05	1.84 ± 0.05	52.87 ± 0.016	Long
080310	2.42	46.72 ± 0.11	4.08 ± 0.11	52.88 ± 0.023	Long
080430	0.77	46.03 ± 0.08	4.29 ± 0.08	51.68 ± 0.022	Long
080603B	2.69	48.88 ± 0.26	2.92 ± 0.24	53.07 ± 0.011	Long
080810	3.35	48.24 ± 0.08	3.28 ± 0.07	53.42 ± 0.031	Long
081008	1.97	47.79 ± 0.24	2.95 ± 0.22	52.85 ± 0.047	Long
090423	8.26	48.48 ± 0.11	2.95 ± 0.1	53.03 ± 0.018	Long

LTE correlation



Xu & Huang 2011

LT vs LTE

H=69.7, Ω_M=0.291

LT: $\text{Log}[\text{L}/10^{47}\text{erg/s}] = 0.78_{[\pm 0.14]} - 1.16_{[\pm 0.16]} \text{Log}[\text{T}/10^3\text{s}]$

r=-0.73, P=5.6×10⁻⁸

σ_{int}=0.85±0.10

LTE关系比LT关系更紧密

LTE: $\text{Log}[\text{L}/10^{47}\text{erg/s}] = 1.17_{[\pm 0.09]} - 0.87_{[\pm 0.09]} \text{Log}[\text{T}/10^3\text{s}] + 0.88_{[\pm 0.08]} \text{Log}[\text{E}_\text{iso}/10^{53}\text{erg}]$

r=0.92, P=1.05×10⁻²⁰

σ_{int}=0.43±0.05



Statistical Study of Gamma-Ray Bursts with a Plateau Phase in the X-Ray Afterglow

Chen-Han Tang¹, Yong-Feng Huang^{1,2} , Jin-Jun Geng¹ , and Zhi-Bin Zhang³

¹ School of Astronomy and Space Science, Nanjing University, Nanjing 210023, People's Republic of China; hyf@nju.edu.cn, gengjinjun@nju.edu.cn

² Key Laboratory of Modern Astronomy and Astrophysics (Nanjing University), Ministry of Education, People's Republic of China

³ College of Physics and Engineering, Qufu Normal University, Qufu 273165, People's Republic of China

Received 2019 May 18; revised 2019 September 6; accepted 2019 September 17; published 2019 October 22

Abstract

A plateau phase in the X-ray afterglow is observed in a significant fraction of gamma-ray bursts (GRBs). Previously, a correlation among three key parameters concerning the plateau phase is found to exist, i.e., the end time of the plateau phase in the GRB rest frame (T_a), the corresponding X-ray luminosity at the end time (L_X) and the isotropic energy of the prompt GRB ($E_{\gamma,\text{iso}}$). In this study, we systematically search through all the *Swift* GRBs with a plateau phase that occurred between 2005 May and 2018 August. We collect 174 GRBs, with redshifts available for all of them. For the whole sample, the correlation between L_X , T_a , and $E_{\gamma,\text{iso}}$ is confirmed, with the best-fit relation being $L_X \propto T_a^{-1.01} E_{\gamma,\text{iso}}^{0.84}$. Such an updated three-parameter correlation still supports that the central leftover after GRBs is probably a millisecond magnetar. Note that short GRBs with durations less than 2 s in our sample also follow the same correlation, which hints that the merger production of two neutron stars could be a high-mass magnetar but not necessarily a black hole. Moreover, GRBs with an “internal” plateau (i.e., with a following decay index being generally smaller than -3) also obey this correlation. It further strengthens the idea that the internal plateau is due to the delayed collapse of a high-mass neutron star into a black hole. The updated three-parameter correlation indicates that GRBs with a plateau phase may act as a standard candle for cosmology study.

Key words: gamma-ray burst: general – methods: statistical

Supporting material: extended figure

Sample selectoin

- Swift GRBs with a plateau phase
- Plateau phase well defined by data
- between 2005 May and 2018 August
- the power-law index -1 ----- +1
- no flares during the plateau phase
- redshift available
- 174 GRBs

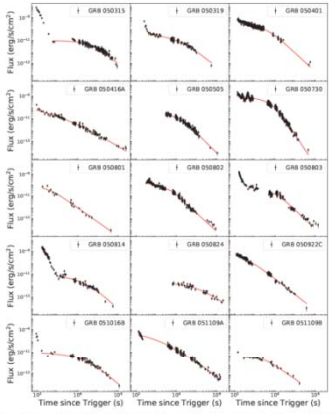


Figure 1. Observed X-ray光子流 of all the 714 GRBs in our sample, and our best fit to the light curve. Black dots correspond to the observational data by Swift/XRT (Evans et al. 2007, 2009). The data fit is preferred with the Markov Chain Monte Carlo (MCMC) algorithm.

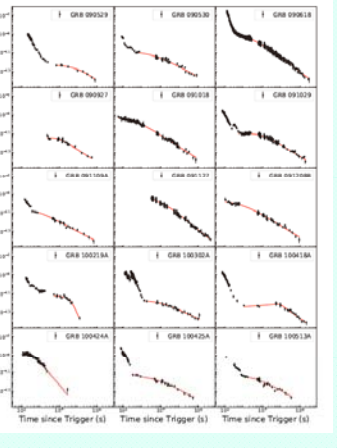
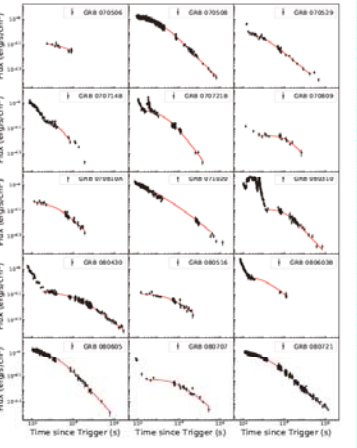
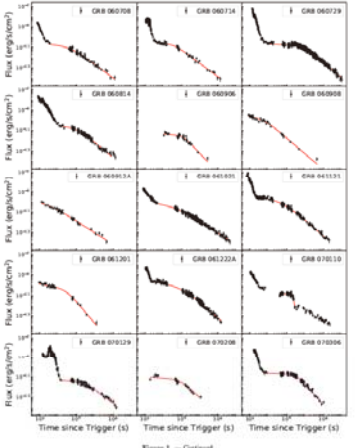
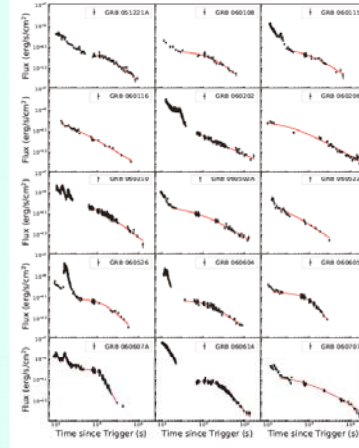


Figure 1. — Continued

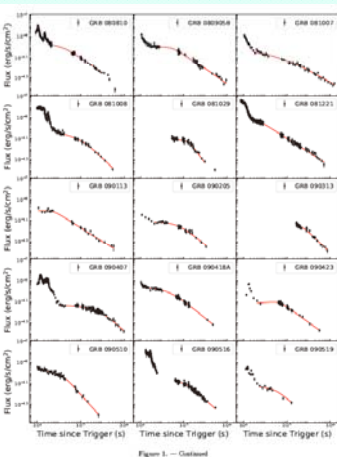
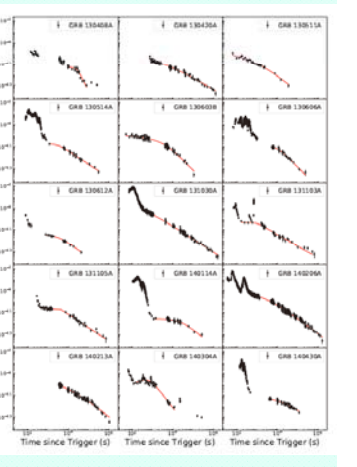
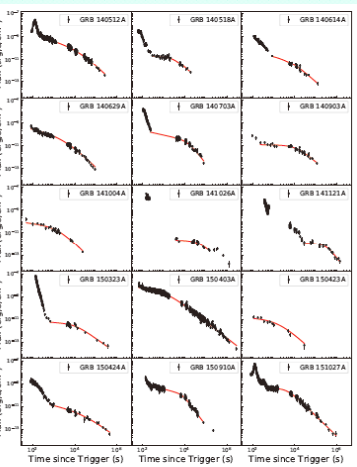
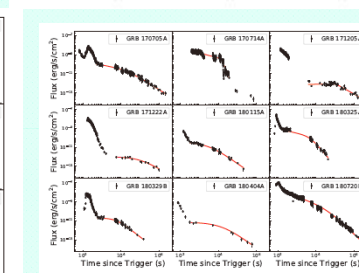
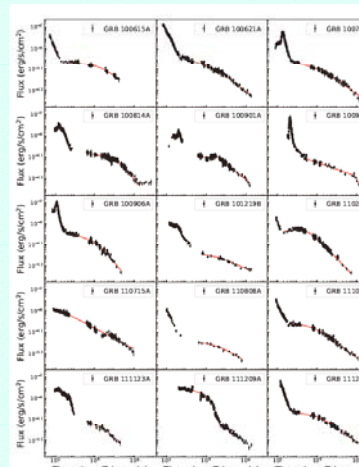


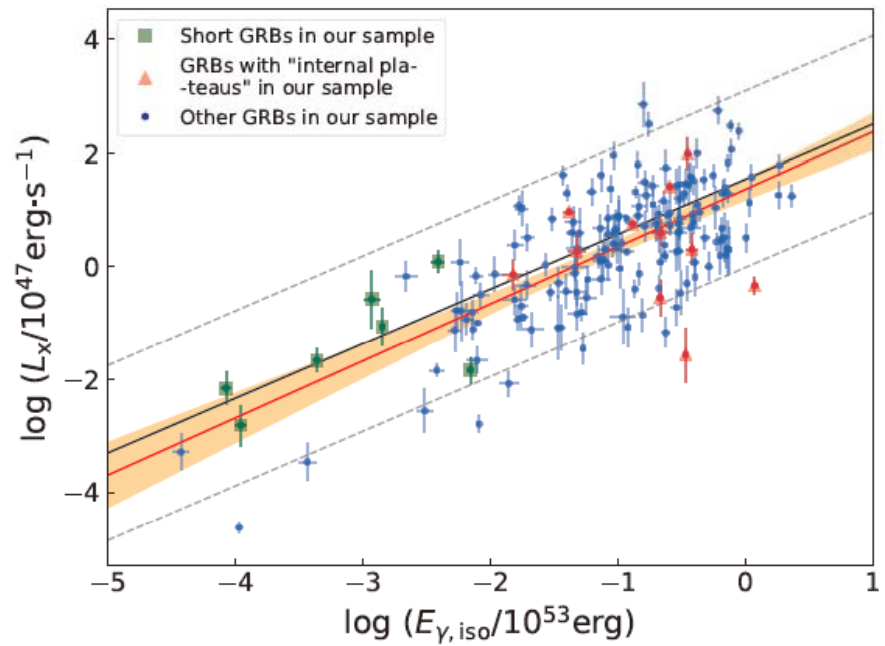
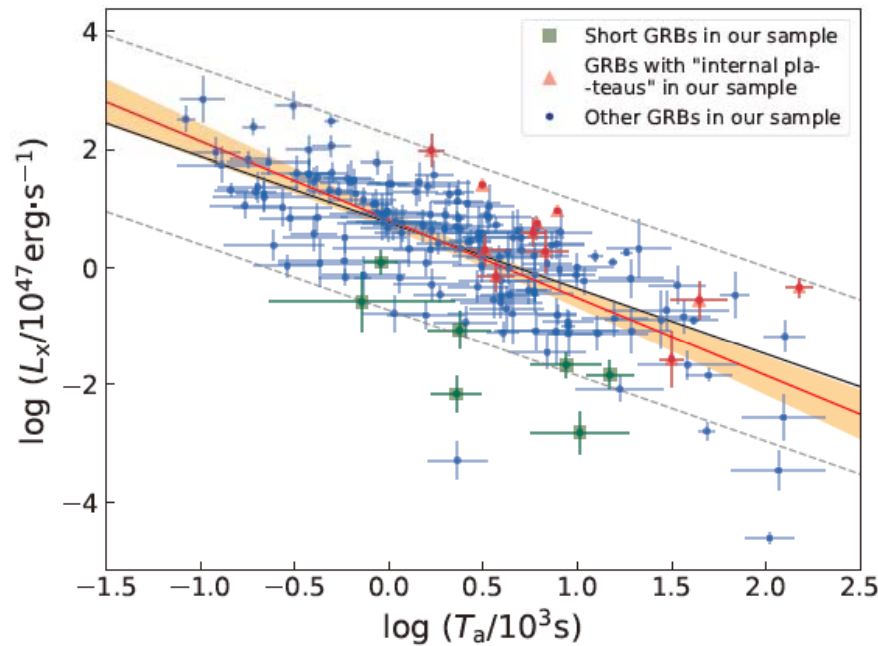
Figure 1. — Continued



174 GRBs in: Tang, Huang, Geng, Zhang, 2019, ApJS, 245, 1

Table 3. Fitting Results and Some Key Parameters of the 174 GRBs in Our Sample

GRB Name	T_{90}^a	z^a	$S(15\text{-}150 \text{ keV})^a$	α_1^b	α_2^b	$\log(T_{90}/10^{30})^b$	$\log(L_X/10^{42})^c$	$\log(E_{\gamma,\text{iso}}^r/10^{53})^d$	$\log(E_{\gamma,\text{iso}}/10^{53})^e$
	(s)		(10^{-7} erg/cm 2)			(s)	(erg/s)	(erg)	(erg)
GRB 060315	95.6	1.949	32.2 ± 1.46	-0.03 ± 0.06	1.94 ± 0.26	1.63 ± 0.15	-0.29 ± 0.32	-0.62 ± 0.02	-0.46 ± 0.02
GRB 060319	152.5	3.24	13.1 ± 1.48	0.15 ± 0.11	1.41 ± 0.17	0.53 ± 0.22	0.86 ± 0.27	-0.53 ± 0.06	-0.52 ± 0.06
GRB 060401	33.3	2.9	82.2 ± 3.06	0.55 ± 0.03	1.63 ± 0.28	0.21 ± 0.16	1.38 ± 0.17	0.19 ± 0.02	-0.17 ± 0.02
GRB 060416A	2.5	0.6635	3.67 ± 0.37	0.32 ± 0.09	1.09 ± 0.09	0.2 ± 0.2	-0.81 ± 0.22	-2.38 ± 0.04	-2.14 ± 0.04
GRB 060505	58.9	4.27	24.9 ± 1.79	0.06 ± 0.14	1.78 ± 0.11	0.37 ± 0.08	1.29 ± 0.2	-0.06 ± 0.03	-0.49 ± 0.03
GRB 060730	156.5	3.97	23.8 ± 1.52	0.23 ± 0.1	2.77 ± 0.19	0.22 ± 0.07	1.99 ± 0.27	-0.13 ± 0.03	-0.46 ± 0.03
GRB 060801	19.4	1.38	3.1 ± 0.48	0.44 ± 0.45	1.25 ± 0.15	-0.61 ± 0.26	0.38 ± 0.25	-1.81 ± 0.06	-1.81 ± 0.06
GRB 060802	19	1.71	20 ± 1.57	0.5 ± 0.19	1.6 ± 0.08	0.29 ± 0.12	0.67 ± 0.34	-0.82 ± 0.03	-1.02 ± 0.03
GRB 060803	87.9	0.422	21.5 ± 1.35	-0.09 ± 0.11	1.63 ± 0.05	0.95 ± 0.03	-1 ± 0.04	-2.01 ± 0.03	-2.1 ± 0.03
GRB 060814	150.9	5.3	20.1 ± 2.2	0.06 ± 0.14	1.81 ± 0.34	0.66 ± 0.27	0.52 ± 0.43	-0.01 ± 0.05	-0.17 ± 0.05
GRB 060824	22.6	0.83	2.66 ± 0.52	0.05 ± 0.13	1.09 ± 0.23	1.58 ± 0.27	-1.67 ± 0.24	-2.31 ± 0.08	-2.11 ± 0.08
GRB 060922C	4.5	2.199	16.2 ± 0.54	0.61 ± 0.09	1.4 ± 0.07	-0.92 ± 0.13	1.96 ± 0.24	-0.72 ± 0.01	-1.04 ± 0.01
GRB 061016B	4	0.9364	1.7 ± 0.22	0 ± 0.09	1.6 ± 0.18	0.95 ± 0.18	-1.12 ± 0.38	-2.4 ± 0.06	-2.28 ± 0.06
GRB 061109A	37.2	2.346	22 ± 2.72	0.32 ± 0.08	1.31 ± 0.05	-0.19 ± 0.11	1.49 ± 0.19	-0.54 ± 0.06	-0.8 ± 0.06
GRB 061109B	14.3	0.08	2.56 ± 0.41	-0.02 ± 0.15	1.35 ± 0.16	0.36 ± 0.15	-3.29 ± 0.32	-4.43 ± 0.06	-4.43 ± 0.06
GRB 061221A	1.4	0.547	11.5 ± 0.35	0 ± 0.22	1.43 ± 0.11	1.17 ± 0.12	-1.84 ± 0.23	-2.04 ± 0.01	-2.16 ± 0.01
GRB 060108	14.3	2.03	3.69 ± 0.37	0.14 ± 0.13	1.46 ± 0.22	0.77 ± 0.2	-0.43 ± 0.31	-1.42 ± 0.04	-1.41 ± 0.04
GRB 060115	139.6	3.53	17.1 ± 1.5	0.22 ± 0.18	1.28 ± 0.17	0.38 ± 0.16	0.33 ± 0.28	-0.35 ± 0.04	-1.01 ± 0.04
GRB 060116	106.9	4	24.1 ± 2.61	0.63 ± 0.24	1.2 ± 0.17	-0.66 ± 0.27	1.2 ± 0.25	-0.12 ± 0.04	-0.52 ± 0.04
GRB 060202	198.9	0.78	21.3 ± 1.65	-0.08 ± 0.29	0.88 ± 0.03	0.27 ± 0.14	-0.45 ± 0.14	-1.46 ± 0.03	-1.53 ± 0.03
GRB 060206	7.6	4.05	8.31 ± 0.42	0.22 ± 0.17	1.03 ± 0.07	-0.49 ± 0.19	1.61 ± 0.27	-0.57 ± 0.02	-1.14 ± 0.02
GRB 060210	255	3.91	76.6 ± 4.09	0.07 ± 0.16	1.47 ± 0.08	0.24 ± 0.1	1.58 ± 0.22	0.37 ± 0.02	0.04 ± 0.02
GRB 060502A	28.4	1.51	23.1 ± 1.02	0.2 ± 0.11	1.18 ± 0.08	0.49 ± 0.15	0.03 ± 0.26	-0.86 ± 0.02	-1.08 ± 0.02
GRB 060522	71.1	5.11	11.4 ± 1.11	0.48 ± 0.35	1.32 ± 0.17	-0.89 ± 0.24	1.74 ± 0.3	-0.28 ± 0.04	-0.63 ± 0.04
GRB 060626	298.2	3.21	12.6 ± 1.65	0.09 ± 0.17	1.85 ± 0.28	0.63 ± 0.18	0.27 ± 0.35	-0.55 ± 0.06	-0.55 ± 0.06
GRB 060604	95	2.1357	4.02 ± 1.06	0.04 ± 0.17	1.32 ± 0.11	0.64 ± 0.14	-0.01 ± 0.24	-1.35 ± 0.1	-1.34 ± 0.1
GRB 060605	79.1	3.8	6.97 ± 0.9	0.17 ± 0.12	2.56 ± 0.27	0.3 ± 0.11	0.9 ± 0.27	-0.69 ± 0.06	-1 ± 0.06
GRB 060607A	102.2	3.082	25.5 ± 1.12	0.47 ± 0.02	3.47 ± 0.1	0.5 ± 0.01	1.41 ± 0.02	-0.28 ± 0.02	-0.6 ± 0.02
GRB 060614	108.7	0.13	204 ± 3.63	-0.02 ± 0.05	2.19 ± 0.13	1.69 ± 0.04	-2.79 ± 0.15	-2.09 ± 0.01	-2.09 ± 0.01
GRB 060707	66.2	3.43	16 ± 1.51	0.13 ± 0.14	1.28 ± 0.16	0.47 ± 0.27	0.59 ± 0.44	-0.4 ± 0.04	-1.31 ± 0.04
GRB 060708	10.2	2.3	4.94 ± 0.37	0.1 ± 0.16	1.33 ± 0.1	0.07 ± 0.14	0.6 ± 0.25	-1.2 ± 0.03	-1.37 ± 0.03
GRB 060714	115	2.71	28.3 ± 1.67	0.13 ± 0.15	1.31 ± 0.06	-0.01 ± 0.1	0.97 ± 0.16	-0.32 ± 0.02	-0.36 ± 0.02
GRB 060729	115.3	0.54	26.1 ± 2.11	0.05 ± 0.04	1.44 ± 0.02	1.62 ± 0.02	-0.9 ± 0.06	-1.7 ± 0.03	-1.75 ± 0.03
GRB 060814	145.3	0.84	146 ± 2.39	0.1 ± 0.17	1.51 ± 0.08	0.74 ± 0.1	-0.38 ± 0.22	-0.56 ± 0.01	-0.68 ± 0.01
GRB 060906	43.5	3.685	22.1 ± 1.36	0.18 ± 0.14	1.93 ± 0.4	0.43 ± 0.11	0.46 ± 0.19	-0.21 ± 0.03	-0.19 ± 0.03
GRB 060908	19.3	1.8836	28 ± 1.11	0.25 ± 0.19	1.56 ± 0.18	-0.7 ± 0.21	1.37 ± 0.25	-0.6 ± 0.02	-1.06 ± 0.02
GRB 060912A	5	0.937	13.5 ± 0.62	0.5 ± 0.2	1.14 ± 0.06	-0.54 ± 0.18	0.03 ± 0.19	-1.5 ± 0.02	-1.57 ± 0.02



$$L_X \propto T_a^{-1.01} E_{\gamma, \text{iso}}^{0.84}$$

$$L_X \propto T_a^{-0.87} E_{\gamma, \text{iso}}^{0.88}$$

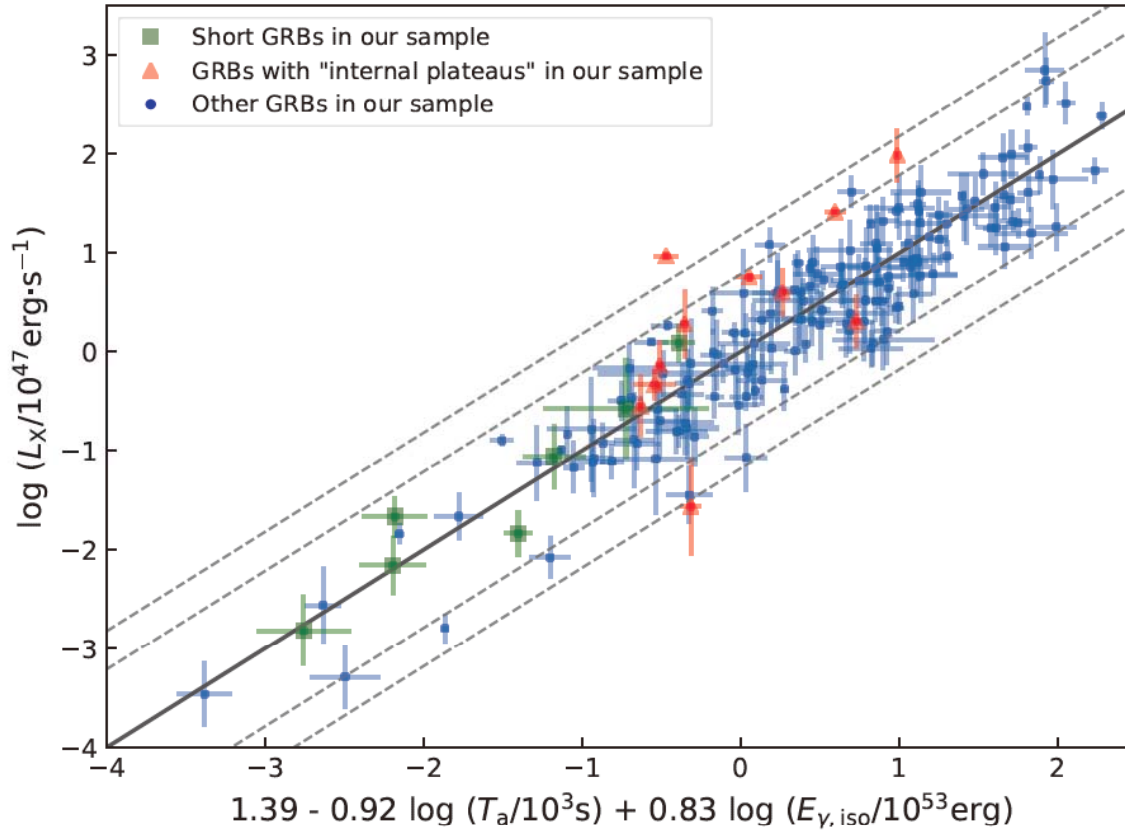


Figure 8. The best-fit L-T-E correlation by using all the 174 GRBs of our sample. Here, L_X is the luminosity at the end time of the plateau, T_a is the corresponding end time, and $E_{\gamma, \text{iso}}$ is the isotropic γ -ray energy of the prompt emission. The black solid lines are the best fit for the observational data points. The black dashed lines are error lines of 2σ and 3σ confidence intervals.

$$\log(L_X/10^{47} \text{erg}\cdot\text{s}^{-1}) = (1.11 \pm 0.04) + (-1.01 \pm 0.05) \log(T_a/10^3 \text{s}) + (0.84 \pm 0.04) \log(E_{\gamma, \text{iso}}/10^{53} \text{erg}).$$

The shallow decay segment of GRB X-ray afterglow revisited

Submitted to APJ 2019 March 9; Accepted 2019 June 27

LITAO ZHAO,¹ BINBIN ZHANG,² HE GAO,³ LIN LAN,⁴ HOUJUN LÜ,⁴ AND BING ZHANG⁵

¹*Department of Astronomy ,Beijing Normal University, Beijing, China;*

²*School of Astronomy and Space Science, Nanjing University, Nanjing 210093, China;*

³*Department of Astronomy , Beijing Normal University, Beijing, China;*

⁴*Guangxi Key Laboratory for Relativistic Astrophysics, Department of Physics, Guangxi University, Nanning 530004, China;*

⁵*Department of Physics and Astronomy, University of Nevada, Las Vegas, NV 89154, USA*

ABSTRACT

Based on the early-year observations from Neil Gehrels *Swift* Observatory, Liang et al. (2007) performed a systematic analysis for the shallow decay component of gamma-ray bursts (GRBs) X-ray afterglow, in order to explore its physical origin. Here we revisit the analysis with an updated sample (with Swift/XRT GRBs between February 2004 and July 2017). We find that with a larger sample, 1) the distributions of the characteristic properties of the shallow decay phase (e.g. t_b , S_X , $\Gamma_{X,1}$, and $\alpha_{X,1}$) still accords with normal or lognormal distribution; 2) $\Gamma_{X,1}$ and Γ_γ still show no correlation, but the tentative correlations of durations, energy fluences, and isotropic energies between the gamma-ray and X-ray phases still exist; 3) for most GRBs, there is no significant spectral evolution between the shallow decay segment and its follow-up segment, and the latter is usually consistent with the external-shock models; 4) assuming that the central engine has a power-law luminosity release history as $L(t) = L_0(\frac{t}{t_0})^{-q}$, we find that the value q is mainly distributed between -0.5 and 0.5, with an average value of 0.16 ± 0.12 ; 5) the tentative correlation between $E_{\text{iso},X}$ and t'_b disappears, so that the global 3-parameter correlation ($E_{\text{iso},X} - E'_p - t'_b$) becomes less significant; 6) the anti-correlation between L_X and t'_b and the three-parameter correlation ($E_{\text{iso},\gamma} - L_X - t_b$) indeed exist with a high confidence level. Overall, our results are generally consistent with Liang et al. (2007), confirming their suggestion that the shallow decay segment in most bursts is consistent with an external forward shock origin, probably due to a continuous energy injection from a long-lived central engine.

1. INTRODUCTION

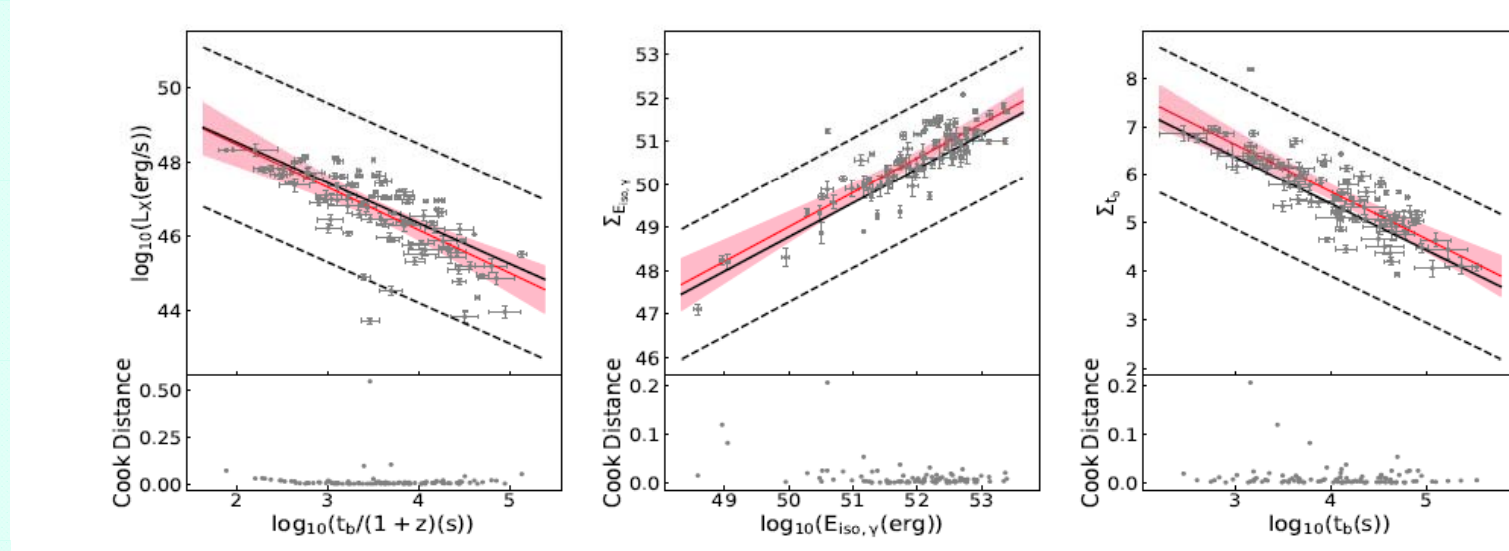
Gamma-ray bursts (GRBs) are considered as the most extreme explosive events in the universe, which contains two phenomenological emission phases: prompt phase (with an initial prompt γ -ray emission) and afterglow phase (with a longer-lived broadband emission) (Zhang 2019). Although there are many uncertainties in the detailed physics of the prompt emission, mainly due to our poorly understanding the degree of magnetization of the GRB jet (Zhang 2014a; Kumar & Zhang 2015) a generic synchrotron external shock model has been constructed for interpreting the

The shallow decay segment of GRB X-ray afterglow revisited

201 GRBs

Submitted to APJ 2019 March 9; Accepted 2019 June 27

LITAO ZHAO,¹ BINBIN ZHANG,² HE GAO,³ LIN LAN,⁴ HOUJUN LÜ,⁴ AND BING ZHANG⁵



$$L_X \propto T_a^{-0.97} E_{\gamma,\text{iso}}^{0.79}$$

$$L_X \propto T_a^{-0.87} E_{\gamma,\text{iso}}^{0.88}$$

$$L_X \propto T_a^{-1.01} E_{\gamma,\text{iso}}^{0.84}$$



Statistical properties of the X-ray afterglow shallow decay phase and their relationships with the prompt gamma-ray emission of gamma-ray bursts

Xiao-Kang Ding¹ · Yong-Rui Shi¹ · Si-Yuan Zhu¹ · Wan-Peng Sun¹ · Fu-Wen Zhang¹

58 Page 24 of 27

X.-K. Ding et al.

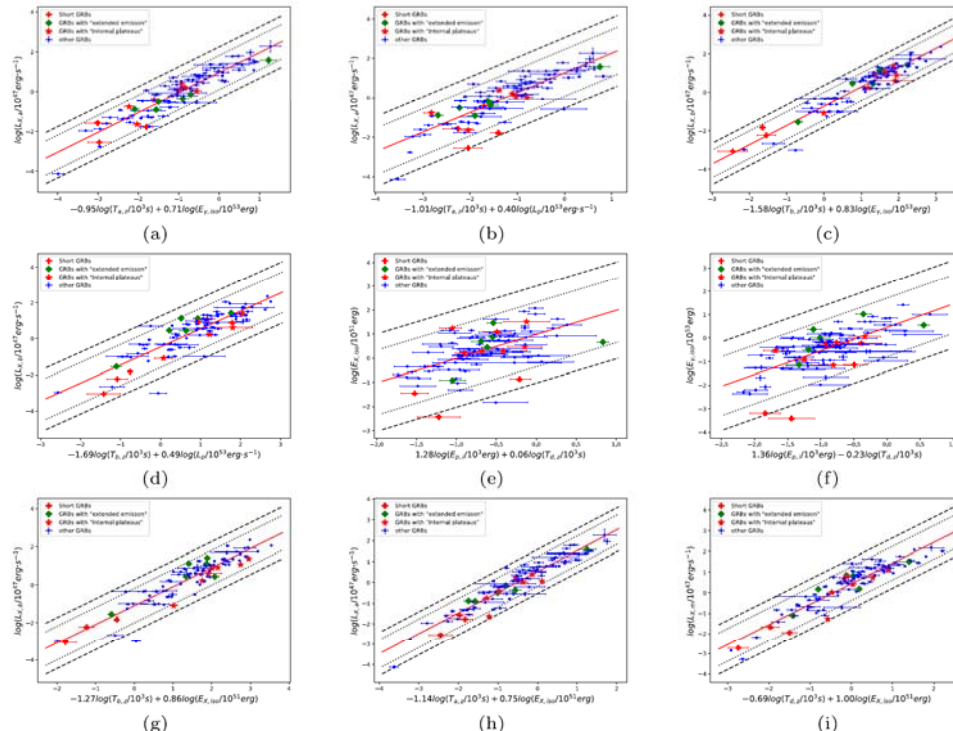


Fig. 8 Three-parameter relationship between the shallow decay phase and the prompt emission. (a) $L_{X,a} - T_{a,z} - E_{\gamma,iso}$, (b) $L_{X,a} - T_{a,z} - L_p$, (c) $L_{X,b} - T_{b,z} - E_{\gamma,iso}$, (d) $L_{X,b} - T_{b,z} - L_p$, (e) $E_{X,iso} - E_{p,i} - T_{d,z}$, (f) $E_{\gamma,iso} - E_{p,i} - T_{d,z}$, (g) $L_{X,b} - T_{d,z} - E_{X,iso}$, (h) $L_{X,a} - T_{d,z} - E_{X,iso}$, (i) $L_{X,m} - T_{d,z} - E_{X,iso}$. The other symbols are the same as Fig. 4

204 GRBs

$$L_{X,b} \propto T_{b,z}^{-1.58 \pm 0.11} E_{\gamma,iso}^{0.83 \pm 0.05}$$

$$L_{X,b} \propto T_{b,z}^{-1.69 \pm 0.16} L_p^{0.49 \pm 0.06}$$



The Three-parameter Correlations About the Optical Plateaus of Gamma-Ray Bursts

Shu-Kun Si¹, Yan-Qing Qi¹, Feng-Xia Xue¹, Ya-Jie Liu¹, Xiao Wu¹, Shuang-Xi Yi¹ ,
Qing-Wen Tang², Yuan-Chuan Zou³ , Fei-Fei Wang³, and Xiang-Gao Wang⁴

¹ School of Physics and Physical Engineering, Shandong Provincial Key Laboratory of Laser Polarization and Information Technology, Qufu Normal University, Qufu 273165, People's Republic of China; yisx2015@qfnu.edu.cn

² Department of Physics, Nanchang University, Nanchang 330031, People's Republic of China; qwtang@ncu.edu.cn

³ School of Physics, Huazhong University of Science and Technology, Wuhan 430074, People's Republic of China; zouyc@hust.edu.cn

⁴ GXU-NAOC Center for Astrophysics and Space Sciences, Department of Physics, Guangxi University, Nanning 530004, People's Republic of China; wangxg@gxu.edu.cn

Received 2018 January 24; revised 2018 June 26; accepted 2018 June 28; published 2018 August 9

Abstract

Well-sampled optical light curves of 50 gamma-ray bursts (GRBs) with plateau features are compiled from the literature. By empirical fitting, we obtained the parameters of the optical plateaus, such as the decay slopes (α_1 and α_2), the break times (T_b), and the corresponding optical fluxes (F_b) at the break times. The break time of optical

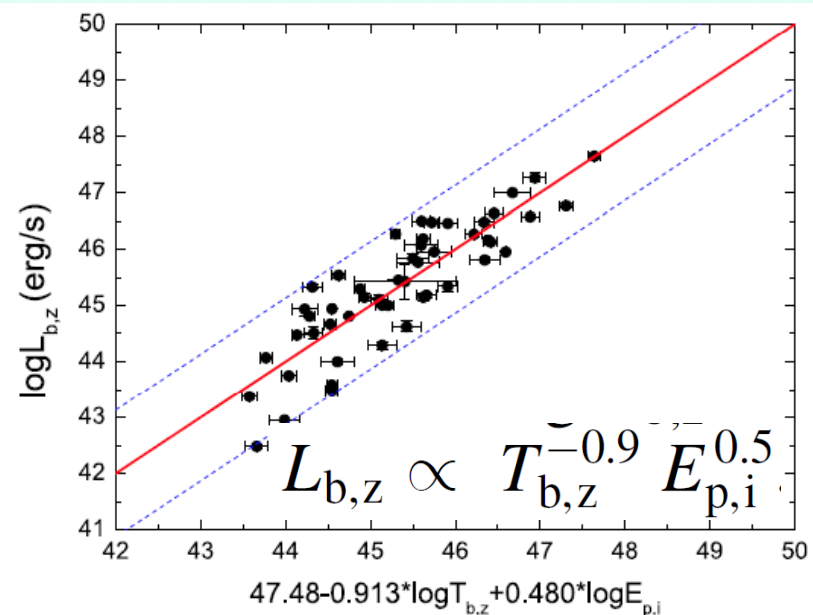
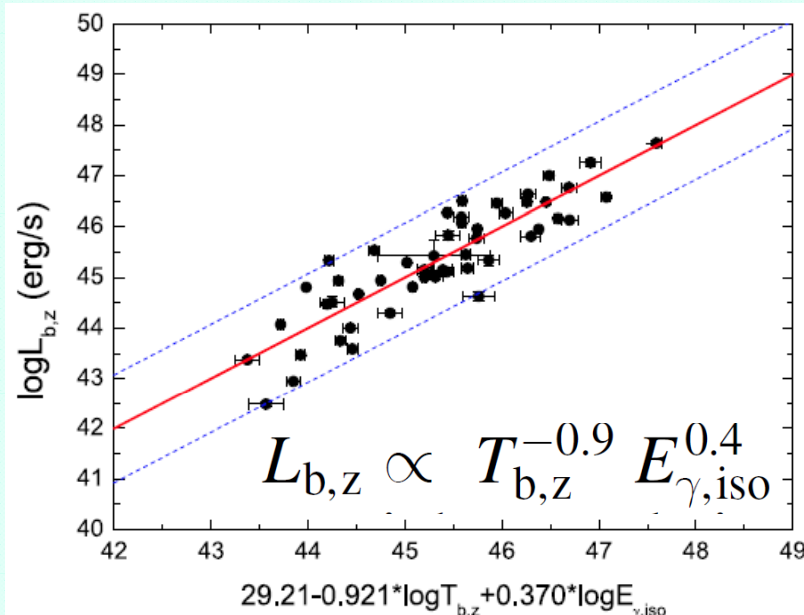
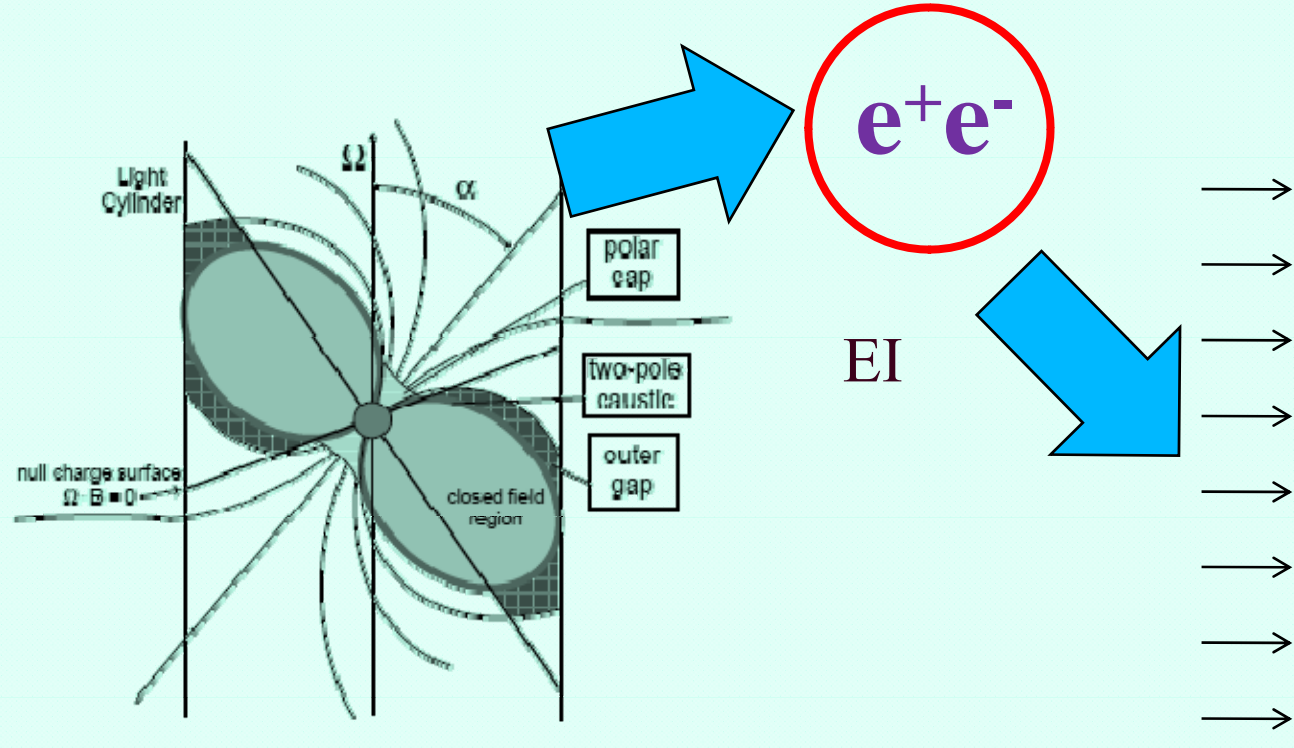


Figure 4. The best fits for two three-parameter correlations.

Support: Energy injection from a magnetar



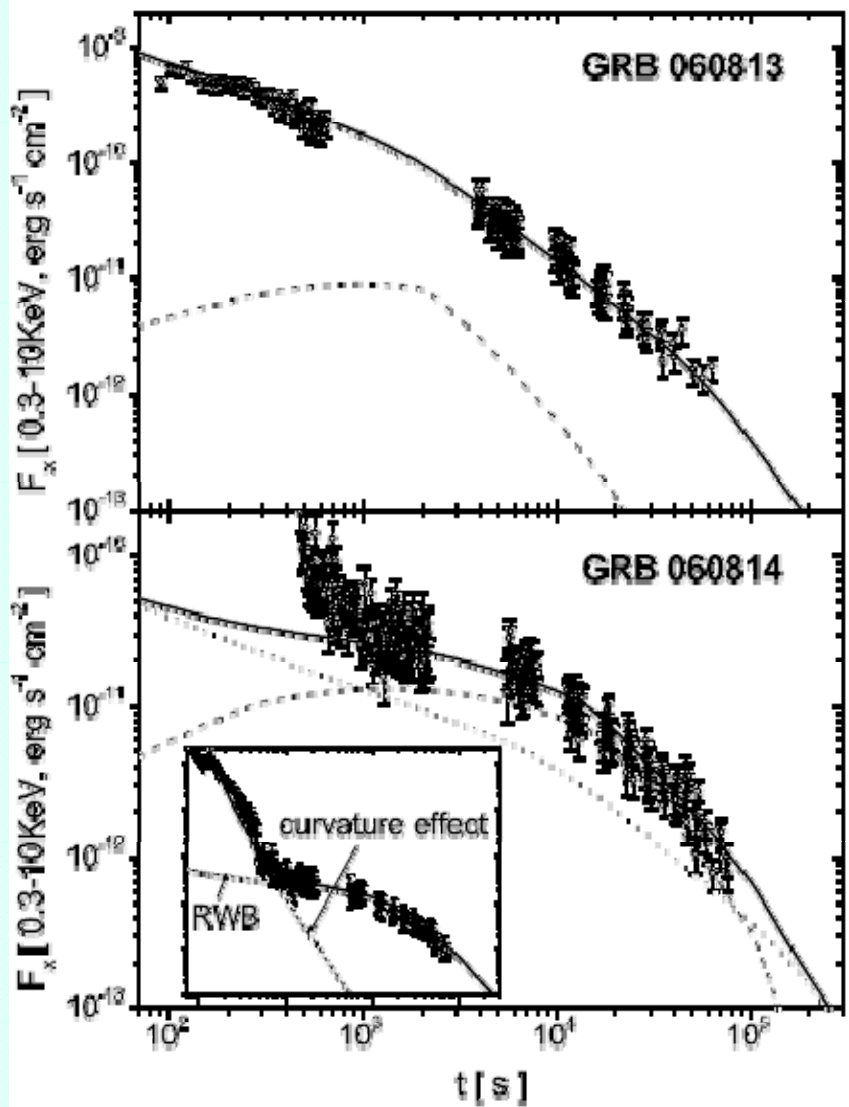
$$L_w \simeq 4 \times 10^{47} B_{\perp,14}^2 R_{M,6}^6 P_{\text{ms}}^{-4} \text{ ergs s}^{-1}$$

Fireball

24

$$L_w \propto \left(1 + \frac{t}{T_{M,0}}\right)^{-2} \begin{cases} \sim \text{const}, & t < T_{M,0} \\ \propto t^{-2}, & t > T_{M,0} \end{cases}$$

Dai 2004



Yu & Dai, 2007

$$E_{\text{injection}} < E_{\text{Fireball}}$$

$$E_{\text{injection}} \geq E_{\text{Fireball}}$$

理论解释：支持磁星能量注入模型

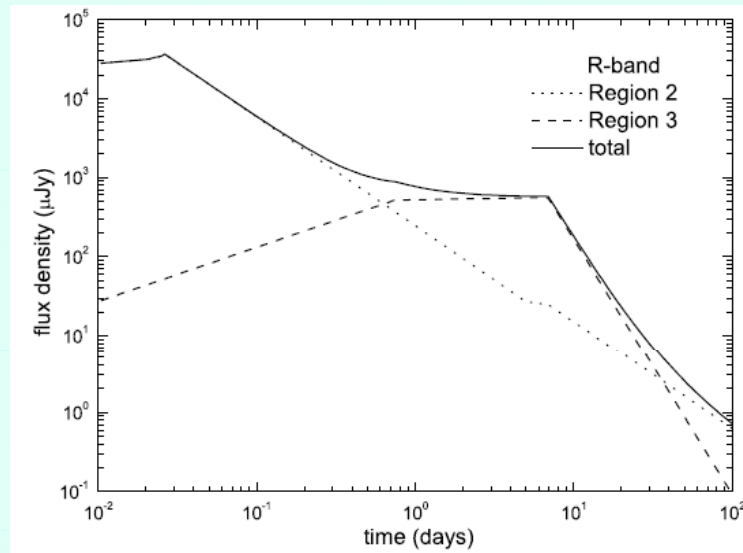
$$L_w \propto \left(1 + \frac{t}{T_{M,0}}\right)^{-2} \begin{cases} \sim \text{const}, & t < T_{M,0} \\ \propto t^{-2}, & t > T_{M,0} \end{cases}$$

$E_{\text{injection}}$

$$L_X T_a$$

$$= \frac{1}{2} I \Omega^2$$

$$\sim E_{\gamma, \text{iso}}$$



Dai 2004

=> L_X - T_a - $E_{\gamma, \text{iso}}$ correlation:

$$L_X \propto T_a^{-1.01} E_{\gamma, \text{iso}}^{0.84}$$

Outline

1. Background

2. Three parameter relation of plateaus

3. Application in cosmology



X-Ray Plateaus in Gamma-Ray Burst Afterglows and Their Application in Cosmology

Fan Xu¹ , Chen-Han Tang¹, Jin-Jun Geng¹ , Fa-Yin Wang^{1,2} , Yu-Yang Wang¹ , Abudushataer Kuerban¹ , and Yong-Feng Huang^{1,2}

¹ School of Astronomy and Space Science, Nanjing University, Nanjing 210023, People's Republic of China; hyf@nju.edu.cn

² Key Laboratory of Modern Astronomy and Astrophysics (Nanjing University), Ministry of Education, People's Republic of China

Received 2020 December 11; revised 2021 July 9; accepted 2021 July 17; published 2021 October 22

Abstract

For gamma-ray bursts (GRBs) with a plateau phase in the X-ray afterglow, a so-called $L-T-E$ correlation that tightly connects the isotropic energy of the prompt GRB ($E_{\gamma,\text{iso}}$) with the end time of the X-ray plateau (T_a) and the corresponding X-ray luminosity at the end time (L_X) has been found. Here we show that there is a clear redshift evolution in the correlation. Furthermore, because the power-law indices of L_X and $E_{\gamma,\text{iso}}$ in the correlation function are almost identical, the $L-T-E$ correlation is insensitive to cosmological parameters and cannot be used as a satisfactory standard candle. On the other hand, based on a sample including 121 long GRBs, we establish a new three-parameter correlation that connects L_X , T_a , and the spectral peak energy E_p , i.e., the $L-T-E_p$ correlation. This correlation strongly supports the so-called Combo-relation established by Izzo et al. After correcting for the redshift evolution, we show that the de-evolved $L-T-E_p$ correlation can be used as a standard candle. By using this correlation alone, we are able to constrain the cosmological parameters as $\Omega_m = 0.389^{+0.202}_{-0.141}$ (1σ) for the flat Λ CDM model, or $\Omega_m = 0.369^{+0.217}_{-0.191}$ and $w = -0.966^{+0.513}_{-0.678}$ (1σ) for the flat w CDM model. Combining with other cosmological probes, more accurate constraints on the cosmology models are presented.

Unified Astronomy Thesaurus concepts: [Cosmology](#) (343); [Cosmological parameters](#) (339); [Dark energy](#) (351); [Dark matter](#) (353); [Gamma-ray bursts](#) (629); [Neutron stars](#) (1108)

LTE关系不能直接用作标准烛光

THE ASTROPHYSICAL JOURNAL, 920:135 (19pp), 2021 October 20

Xu et al.

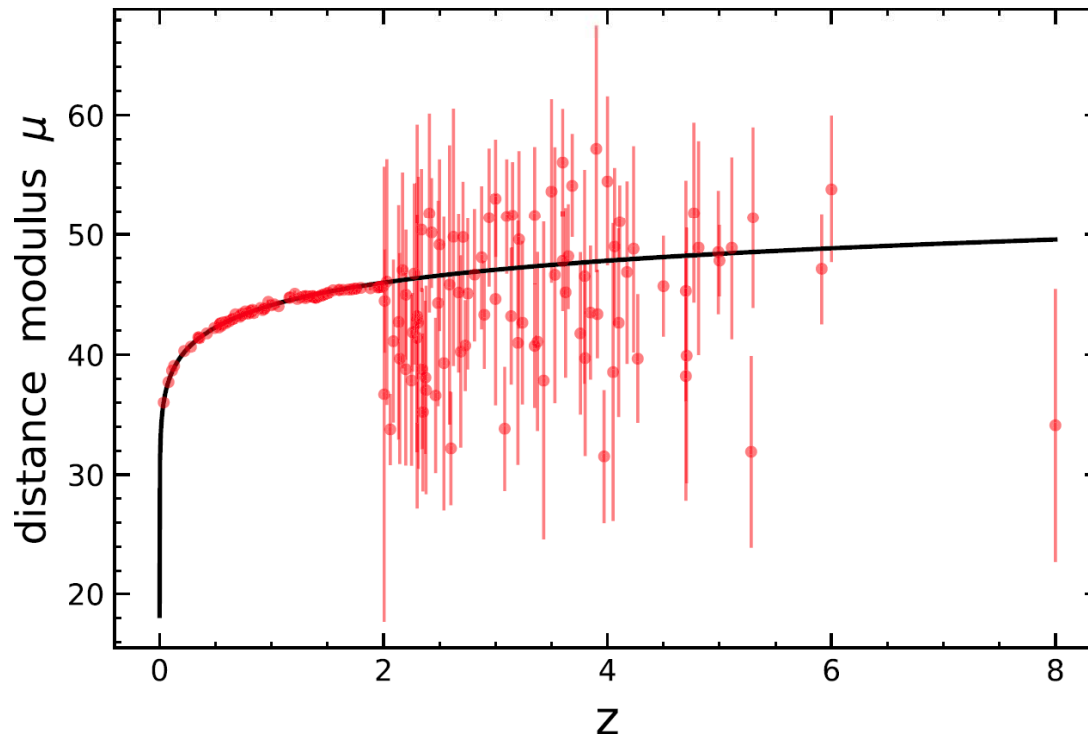


Figure 4. Calibrated GRB Hubble diagram using the $L-T-E$ correlation. The data points represent our GRB sample. As a comparison, the solid curve corresponds to the theoretical distance modules calculated for a flat Λ CDM model with $H_0 = 70.0 \text{ km s}^{-1} \text{ Mpc}^{-1}$ and $\Omega_m = 0.289$.

$$L_X \propto T_a^{-1.01} E_{\gamma, \text{ISO}}^{0.84}$$

29

Xu, Tang, Geng, Wang, Wang, Kuerban, Huang, 2021, ApJ

A new L-T-E_p correlation:

$$L_X \propto T_a^{-0.96} E_p^{0.44}$$

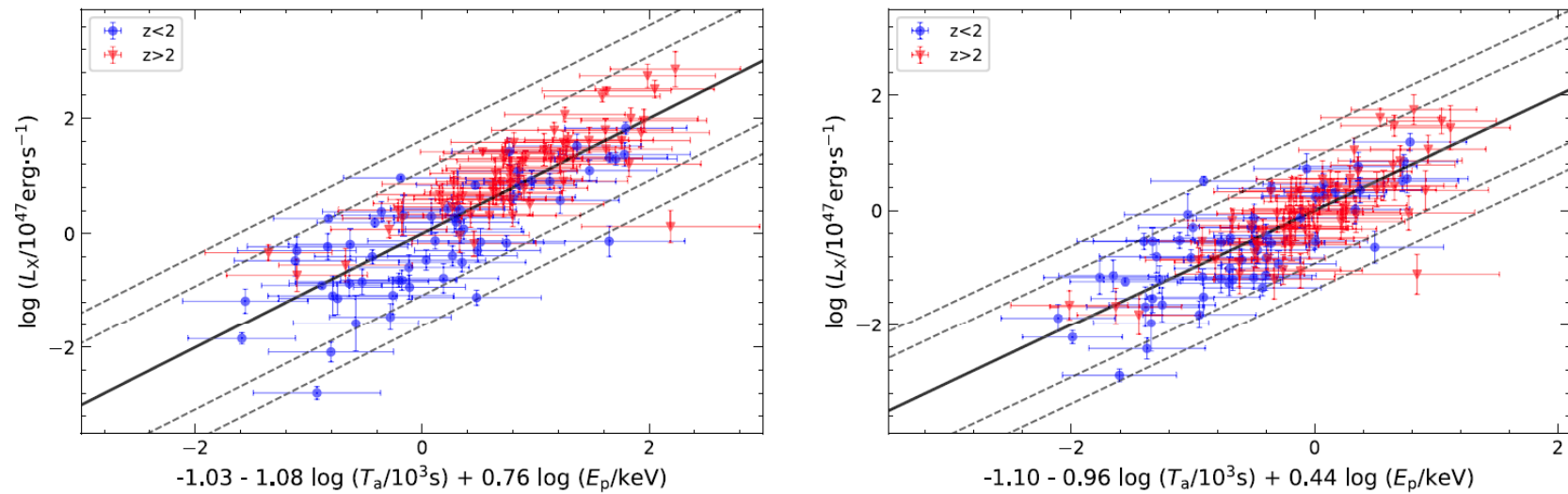
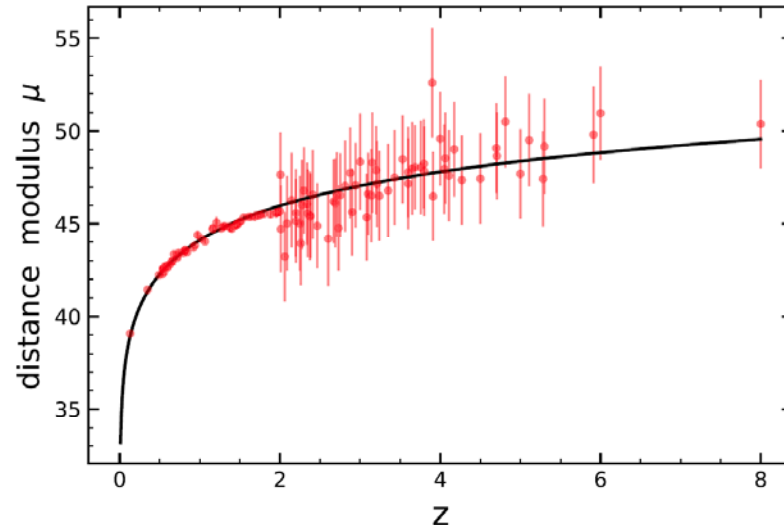


Figure 5. The best-fit result of the $L-T-E_p$ correlation (left panel) and the de-evolved $L-T-E_p$ correlation (right panel). In the left panel, there is a clear systematic deviation between the low-redshift sub-sample and the high-redshift subsample. In the right panel, both subsamples are distributed normally along the best-fit line.



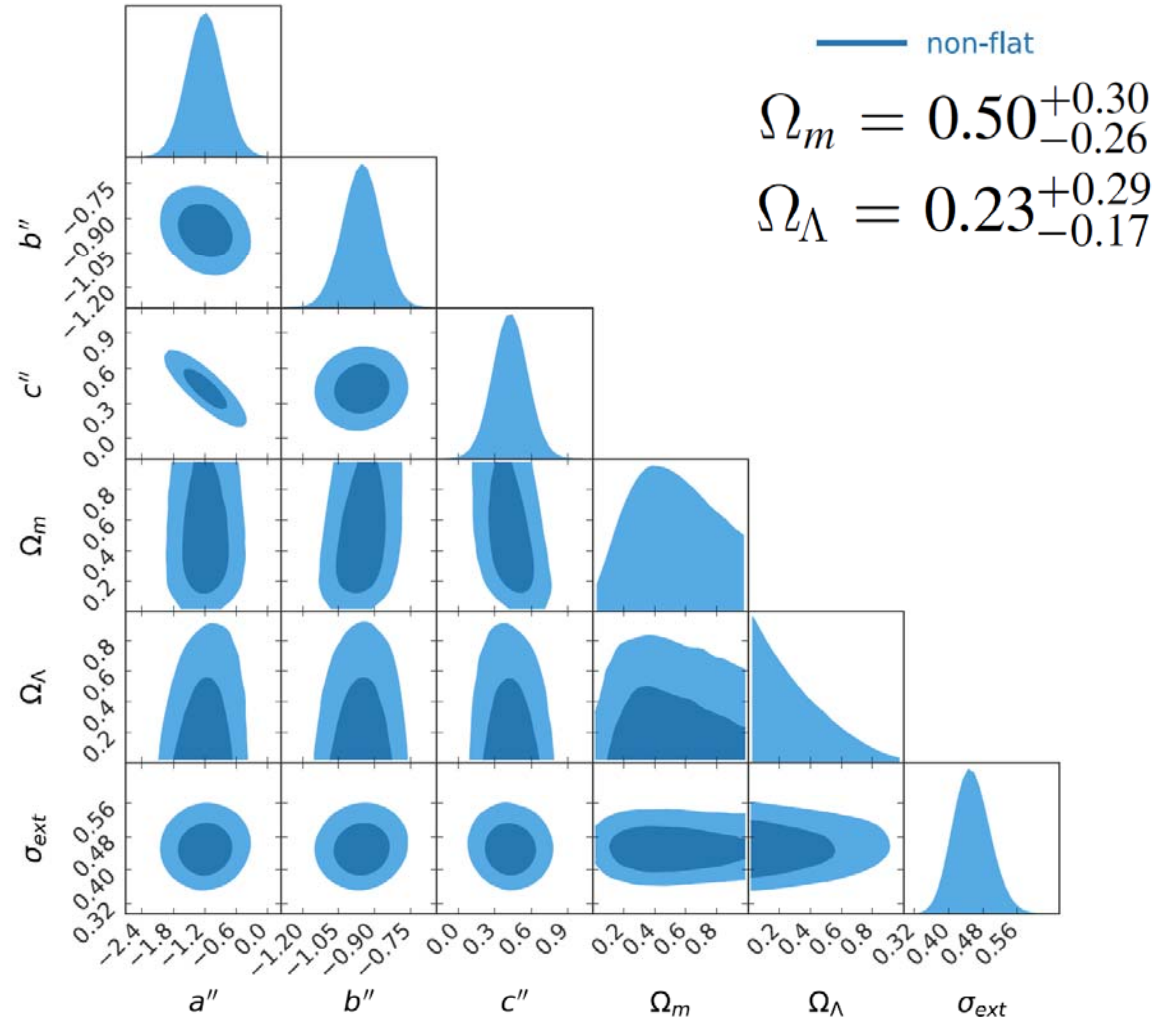
30

Cosmology by using GRBs alone

$$L_X \propto T_a^{-0.96} E_p^{0.44}$$

THE ASTROPHYSICAL JOURNAL, 920:135 (19pp), 2021 October 20

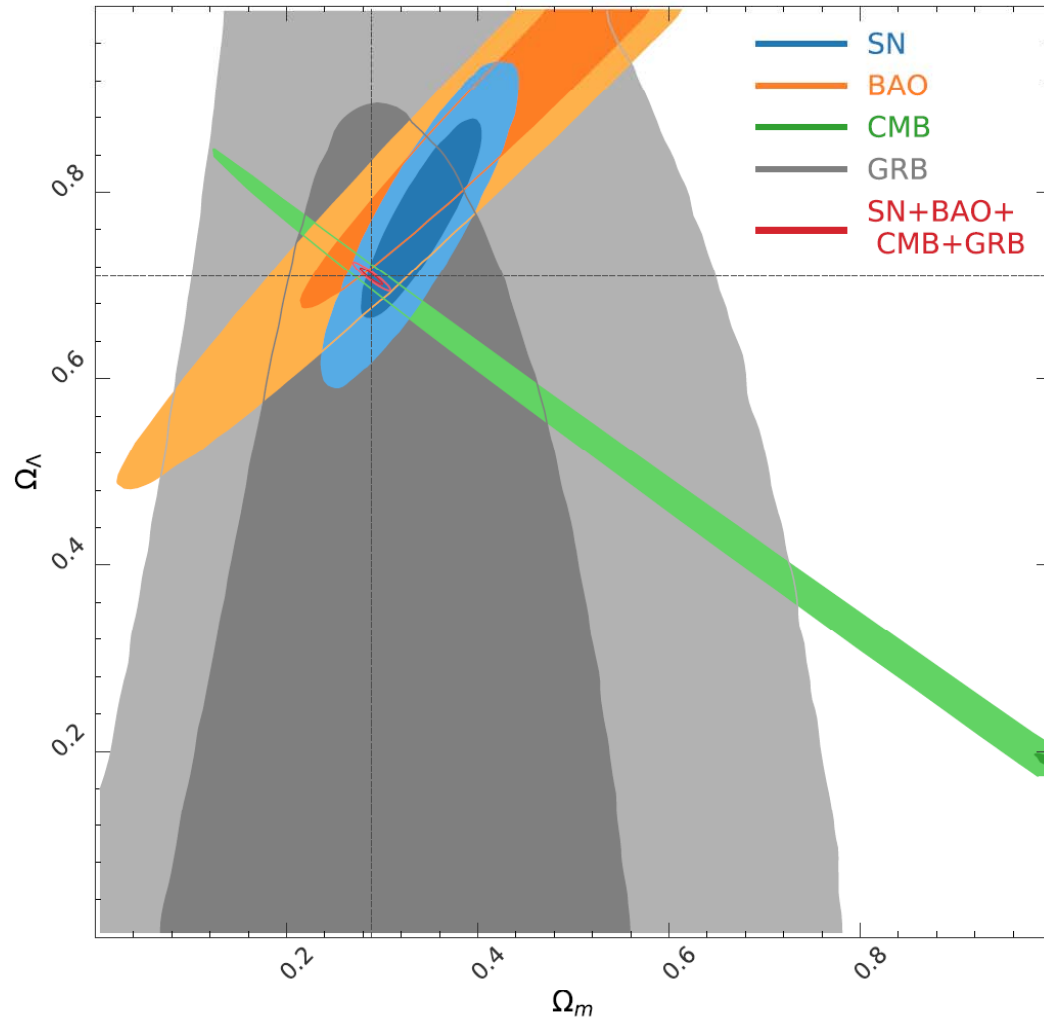
Xu et al.



Cosmology by combining currently available tools

THE ASTROPHYSICAL JOURNAL, 920:135 (19pp), 2021 October 20

Xu et al.



Conclusions

X-ray afterglows with a plateau phase:

- A three parameter relation: LTE

$$L_X \propto T_a^{-1.01} E_{\gamma,iso}^{0.84}$$

- Another 3 parameter relation: LTEp

$$L_X \propto T_a^{-0.96} E_p^{0.44}$$

Thank you!